JOURNAL OF SOLID STATE CHEMISTRY **125,** 54–62 (1996)
ARTICLE NO. 0264

# Continuous Structural Evolution of $(Bi_2O_2)_2V_{2y}O_{4y+2}$ $(1 \leq y \leq 4)$ Aurivillius Phases in the $Bi_2O_3$–$VO_2$ System

Svetlana Sorokina,* Renée Enjalbert,* Pierre Baules,* Alicia Castro,† and Jean Galy*

*Centre d'Elaboration de Matériaux et d'Etudes Structurales, CNRS, 29, rue J. Marvig, 31055 Toulouse Cedex, France; and
†Instituto de Ciencia de Materiales de Madrid, CSIC, Cantoblanco, 28049 Madrid, Spain

Received January 16, 1996; in revised form April 23, 1996; accepted May 2, 1996

**In the $Bi_2O_3$–$VO_2$ system, the series $(Bi_2O_2)_2V_{2y}O_{4y+2}$ with $1 \leq y \leq 4$ has been examined and its structural character determined. The main phase $Bi_4V_2O_{10}$ exhibits three varieties and transformations occur with increasing temperature: $\alpha^{T>690°} \rightarrow \beta^{T>850°} \rightarrow \gamma$. The series of $(Bi_2O_2)_2V_{2y}O_{4y+2}$ showed a typical layered structure built up by alternating $(Bi_2O_2)_n$ layers with $(V_{2y}O_{4y+2})_n$ sheets. These structures have been derived by comparison with the series $CaV_nO_{2n+1}$ where single crystal structures have been established for $CaV_2O_5$, $CaV_3O_7$, and $CaV_4O_9$. The latter phases are models for the particular values $y = 1$, 2, 3, and 4 corresponding to $(Bi_2O_2)_2(VO_3)_2$, $(Bi_2O_2)_2(V_2O_5)_2$, $(Bi_2O_2)_2(V_3O_7)_2$, and $(Bi_2O_2)_2(V_4O_9)_2$, but in contrast to the calcium–vanadium series, there is no definite composition for the $(Bi_2O_2)_2V_{2y}O_{4y+2}$ which evolves gradually from $y = 1$ up to $y = 4$. The environment of both bismuth and vanadium atoms are more or less distorted square pyramids (SP), $VO_5$ and $BiO_4E$ ($E$, lone pair). Correlating with the enrichment of $VO_2$, i.e., with the increasing number of $VO_5$ SP, the layer $V_{2y}O_{4y+2}$ shows a continuous densification, the $VO_5$ SP sharing an increasing number of edges, compatible with the organization governed by the $(Bi_2O_2)_n$ Aurivillius layer.** 

## INTRODUCTION

The present work is part of our program concerning the structural and physical studies of compounds containing lone pair $ns^2$ metals (1–3) and/or mixed valence oxides particularly with a vanadium element (4). Recently, Galy *et al.* (5) designed and synthesized $Bi_4V_2O_{10}$ or $(Bi_2O_2)_2V_2O_6$, a new Aurivillius phase which exhibits a typical layered structure, $(Bi_2O_2)_n$ layers alternating with $(VO_3)_n$ ones. The $(VO_3)_n$ layers are built up by $VO_5$ SP (square pyramids) sharing their basal corners. Similar layers built up from $VO_5$ units (vanadium $V^{4+}$) have been found by Bouloux and Galy (6, 7) in a remarkable structurally related family $CaV_nO_{2n+1}$ ($n$ being an integer equal to 2, 3, and 4). These vanadates IV, $CaV_2O_5$, $CaV_3O_7$, $CaV_4O_9$, are definite compounds accompanied by other phases like $SrV_3O_7$, $CdV_3O_7$ (7, 8), or again $Rb_2V_4O_9$, and $Cs_2V_4O_9$ (9). It was assumed that for the member $n = 1$ of the series, i.e., $CaVO_3$, instead of a classical perovskite structure, the structure could exhibit a layer $(VO_3)_n$ of $VO_5$ SP sandwiching a calcium layer. Such arrangement is found in $Bi_4V_2O_{10}$ or $(Bi_2O_2)_2(VO_3)_2$, where the $(Bi_2O_2)_n$ layer has been substituted for the calcium layer.

So, it was very tempting to comtemplate the possibility of obtaining condensed $VO_5$ SP layers between the $(Bi_2O_2)_n$ layers by adding the $VO_2$ oxide. These investigations support the assumption of phases occurring in the rich $VO_2$ region of the $Bi_2O_3$–$VO_2$ system which has never been systematically studied. Previously, only two compounds have been reported: $Bi_4V_2O_{10}$ (5) and $Bi_2V_3O_9$ (10, 11). $Bi_4V_2O_{10}$ has been identified as an Aurivillius type phase which crystallizes in the orthorhombic system with unit cell parameters $a = 5.494(2)$, $b = 5.504(3)$, $c = 15.449(3)$ Å, space group $P2_122_1$. $Bi_2V_3O_9$ adopts a distorted pyrochlore structure with an orthorhombic cell with $a = 7.04(3)$, $b = 7.55(3)$, $c = 10.70(2)$ Å (10), or $a = 7.622$, $b = 6.977$, $c = 23.35$ Å (11). However while attempting to grow single crystals, Abraham and Mentre (12) showed that this ''compound'' was in actual fact a mixture of two phases: that is, $Bi_{1.7}V_8O_{16}$ and $X$. $Bi_{1.7}V_8O_{16}$ belongs to the hollandite family containing bismuth in the large tunnels of the $[V_8O_{16}]$ framework and crystallizes with the tetragonal symmetry and unit cell parameters $a = 9.930(4)$, $c = 2.914(1)$ Å, space group $I4/m$. The $X$-phase belongs to the tetragonal system, with a body-centered cell and parameters $a = 3.8767$ (5) and $c = 15.337(5)$ Å.

In view of the potential importance of the $Bi_2O_3$–$VO_2$ system, X-ray powder diffraction (XPD), crystal structure investigation, transmission electron microscopy (TEM), and scanning electron microscopy (SEM) have been used to establish the compositional regions and to characterize the phase structure and evolution. The influence of the synthesis conditions on the presence of a phase with differ-



0022-4596/96 $18.00

ent vanadium valences III, IV, and V has also been investigated.

Note that related Aurivillius phases with molybdenum or tungsten are noted: $Bi_4Mo_2O_{12}$ or $Bi_4W_2O_{12}$ and the oxidized phase containing vanadium V(+V): $Bi_4V_2O_{11}$. Formally, its reduction (5) has been formulated $Bi_4V_2O_{11-x}$ with $0 \leq x \leq 1$ thereby yielding, for the upper value $x = 1$, the original compound $Bi_4V_2O_{10}$ which contains only vanadium V(+IV). For clarity, we have chosen variable $y$ to indicate a formula variation in the vanadate IV system, i.e., $(Bi_2O_2)_2V_{2y}O_{4y+2}$ with $1 \leq y \leq 4$.

## EXPERIMENTAL

### *Materials Preparation*

Samples of ternary oxides were synthesized using solid state reactions. Stoichiometric mixtures (according to the formula $2Bi_2O_3 + 2_yVO_2 \rightarrow (Bi_2O_2)_2V_{2y}O_{4y+2}$) of the starting materials $Bi_2O_3$ (99.99%, Aldrich Chem. Co.) and $VO_2$ were weighted in compositions where $1 \leq y \leq 4$. $VO_2$ was prepared by heating an equimolar mixture of $V_2O_5$ and $V_2O_3$ at 850°C for 3 days. $V_2O_3$ itself was obtained by reducing $V_2O_5$ (99,9%, Aldrich Chem. Co.) under hydrogen at 800°C. All the experiments with $VO_2$ and $V_2O_3$ were carried out in sealed evacuated quartz tubes. The samples were heated at different temperatures in the range 650–850°C, for 50 to 100 hr and quenched at room temperature.

### *X-Ray Diffraction*

The phases and their mixtures were checked by X-ray powder diffraction techniques on a Seifert XRD 3000 diffractometer using Cu$K\alpha$ radiation. The cell parameters derived from X-ray powder data were refined through use of the least square techniques. Procedures for single crystal data collection on a CAD4 Enraf–Nonius diffractometer and structural determination have been described elsewhere (5).

### *Electron Diffraction*

Microstructures of the phases were analyzed by SEM on a Cambridge LEICA microscope. The TEM experiments were performed on a Philips CM20 electron microscope with an accelerating voltage of 200 kV and fitted with a TRACOR EDX system. Powder samples were crushed in an agate mortar and deposited on a copper grid capped with a thin carbon layer.

## RESULTS AND DISCUSSION

The systematic study of the $Bi_2O_3$–$VO_2$ system, according to the formula $2Bi_2O_3 + 2yVO_2$ with a continuous enrichment in vanadium dioxide, shows that the phase

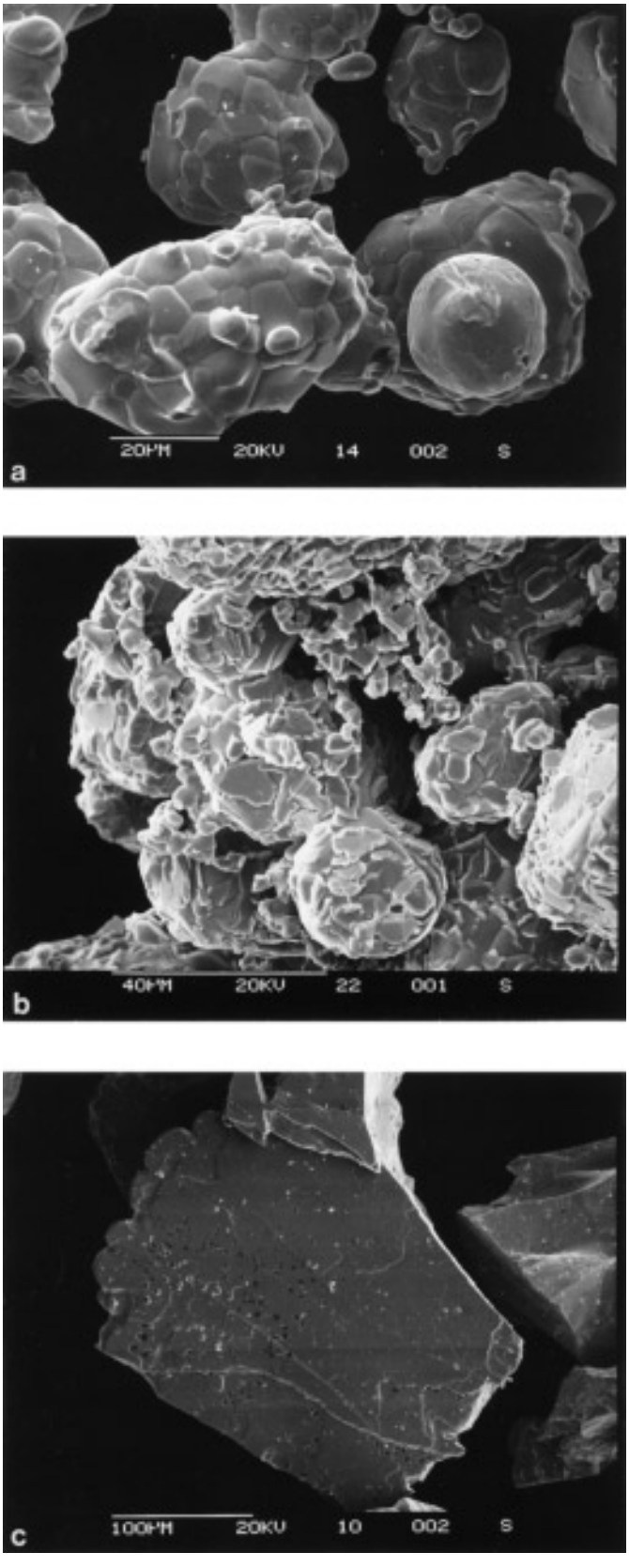


**FIG. 1.** Examples of SEM micrographs of $(Bi_2O_2)_2V_{2y}O_{4y+2}$: (a) $y = 2$ at 650°C, (b) $y = 3$ at 690°C, and (c) $y = 1$ at 890°C.

composition of samples depends on the chosen temperature of reaction. This is indicated by the presence of small amounts of $Bi_{1.66}V_8O_{16}$ and $BiVO_4$ in the samples with $y \geq 1.2$ annealed at temperatures above 700°C, implying the occurrence of an oxido-reduction process. This is overcome in practice at a lower temperature, i.e., between 650 and 700°C, at which temperature the new family of $(Bi_2O_2)_2V_{2y}O_{4y+2}$ phases, with $1 \leq y \leq 4$, has been found.

The $Bi_4V_{2y}O_{4y+6}$ ($y = 1, 2, 3, 4$) samples obtained were examined by SEM to gain better insight into their microstructural evolution as a function of the thermal treatment. In all the samples, crystallites making up spherical particles grow as temperatures increase from 650 to 690°C. Some representative micrographs are shown in Fig. 1. Elongated crystallites can be seen on the grain surface, leading to a small deviation in the spherical shape (Fig. 1a). X-ray diffraction shows the synthesis to occur at 650°C. The process is accelerated when the temperature reaches 690°C (Fig. 1b). Spherical particles made up of small crystallites mixed with plateletlike particles are probably formed as a result of the process started at 650°C by linkage between elongated crystallites. The thermal treatment at $T \geq 700$°C without decomposition was possible only for the $Bi_4V_2O_{10}$ phase or very close $y$ values. In this case, at 890°C, the spherical shape disappears and the initial particles that agglomerated now appear as well-formed platelets (Fig. 1c).

### *$Bi_4V_2O_{10}$ or $(Bi_2O_2)_2(VO_3)_2$*

A special investigation of compositions around the proportions giving the phase $Bi_4V_2O_{10}$ ($2Bi_2O_3 + 2yVO_2$ with $y = 1$) has made it possible to specify more precisely the chemistry and its structural characterization.

The structural evolution of three compositions corresponding to $y = 0.92$, 1, and 1.08 have been analyzed by

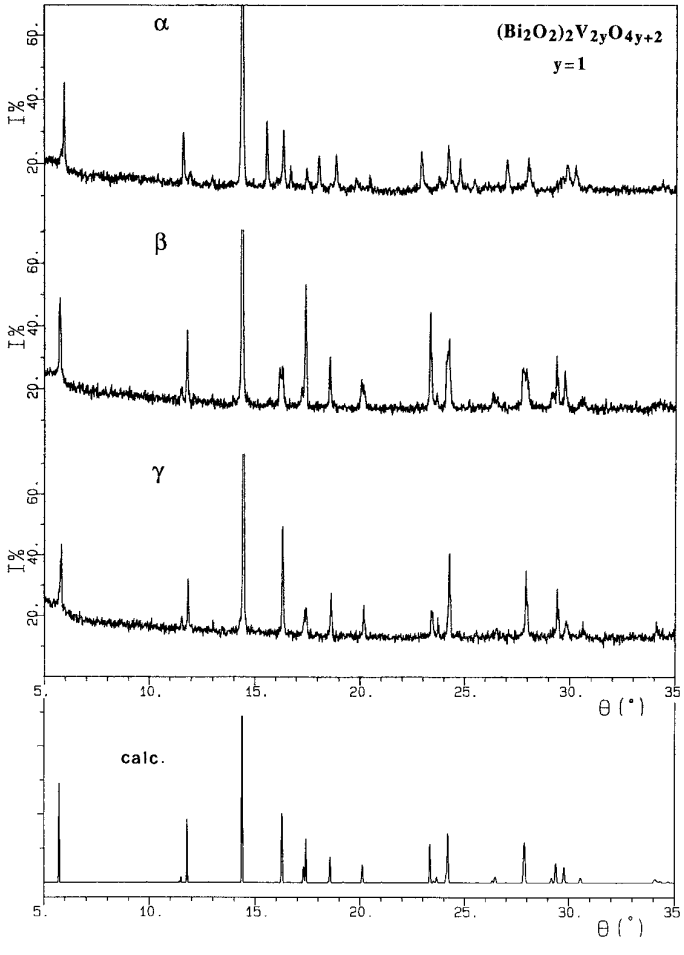


**FIG. 2.** Experimental X-ray powder diffraction patterns of $\alpha$, $\beta$, $\gamma$ polymorphic forms of $Bi_4V_2O_{10}$ and that calculated from the single crystal structure of the $\gamma$ form.

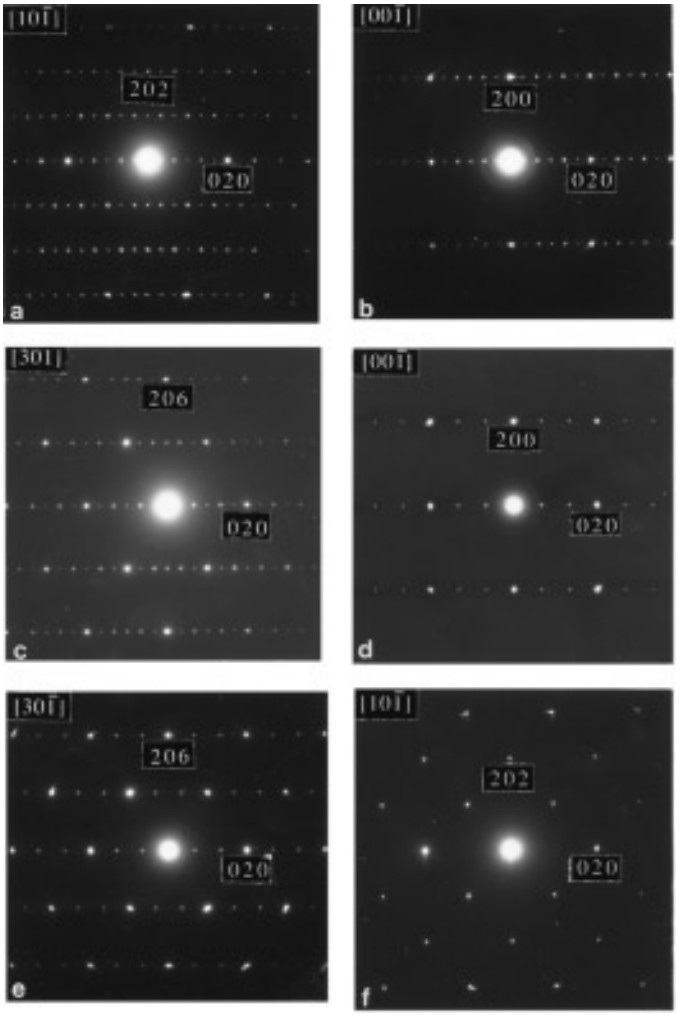


**FIG. 3.** TEM diffraction patterns of the $\alpha$ form (a, b, c), the $\beta$ form (d, e), and the $\gamma$ form (f) of $Bi_4V_2O_{10}$.

**TABLE 1**
**Unit Cell Parameters of the $(Bi_2O_2)_2V_{2y+2}$ Phases in the $Bi_2O_3$–$VO_2$ System**

| $y$ | Formula | Form | $T$(°C) | $a$(Å) | $b$(Å) | $c$(Å) | $V$(Å)$^3$ |
|---|---|---|---|---|---|---|---|
| 0.92 | $Bi_4V_{1.84}O_{9.68}$ | | | | | | |
| | | $\alpha$ | 650 | 5.466(2) | 5.746(2) | 14.918(6) | 468.6(6) |
| | | $\alpha$ | 750 | 5.470(1) | 5.748(1) | 14.929(3) | 469.4(6) |
| | | $\alpha$ | 850 | 5.470(1) | 5.745(1) | 14.939(3) | 469.4(3) |
| 1.0 | $Bi_4V_2O_{10} = (Bi_2O_2)_2(VO_3)_2$ | | | | | | |
| | | $\alpha$ | 650 | 5.471(1) | 5.749(1) | 14.928(2) | 469.5(3) |
| | | $\beta$ | 690 | 5.473(2) | 5.537(2) | 15.473(6) | 468.9(6) |
| | | $\gamma$ | 890 | 5.491(2) | 5.500(3) | 15.459(3) | 467.2(6) |
| | (5) | $\gamma$ | 950 | 5.494(2) | 5.504(3) | 15.449(3) | 467.2(6) |
| 1.08 | $Bi_4V_{1.16}O_{10.32}$ | | | | | | |
| | | $\alpha$ | 650 | 5.471(1) | 5.747(1) | 14.935(3) | 469.5(3) |
| | | $\beta$ | 690 | 5.477(2) | 5.530(3) | 15.479(5) | 468.5(5) |
| | | $\gamma$ | 750 | 5.502(1) | 5.503(1) | 15.476(2) | 468.6(3) |
| 2 | $Bi_4V_4O_{14} = (Bi_2O_2)_2(V_2O_5)_2$ | | 650 | 5.474(1) | 5.527(1) | 15.467(3) | 468.4(3) |
| 3 | $Bi_4V_6O_{16} = (Bi_2O_2)_2(V_3O_7)_2$ | | 650 | 5.481(1) | 5.517(2) | 15.470(3) | 467.8(4) |
| 4 | $Bi_4V_8O_{22} = (Bi_2O_2)_2(V_4O_9)_2$ | | 650 | 5.473(3) | 5.480(5) | 15.465(8) | 463.9(9) |

XPD versus increasing temperature from 650°C (Table 1). The interpretation of the data can be summarized as follows: for $y = 0.92$, the small additional amount of $Bi_2O_3$ stabilizes the $\alpha$ form of $Bi_4V_2O_{10}$ up to 850°C, giving rise to a smooth deviation from the cell parameters obtained for $y = 1$. For $y = 1$, at 650°C $Bi_4V_2O_{10}$ exhibits an orthorhombic structure $\alpha$ that subsequently gives rise at a higher temperature to two successive orthorhombic forms $\beta$ and $\gamma$ (Fig. 2):

$$\alpha\,Bi_4V_2O_{10} \xrightarrow{T>690°C} \beta\,Bi_4V_2O_{10} \xrightarrow{T>850°C} \gamma\,Bi_4V_2O_{10}.$$

For $y = 1.08$, the sample is already in the homogeneity range of the series $Bi_4V_{2y}O_{4y+6}$ and behaves as the composition $y = 1$, but the temperature of the phase transition $\beta \rightarrow \gamma$ is lowered to 750°C.

Electron diffraction micrographs of these phases, obtained by TEM, are shown in Fig. 3. The $\alpha$ phase appears in the $(10\bar{1})^*$, $(00\bar{1})^*$, and $(30\bar{1})^*$ planes (Figs. 3a, 3b, and 3c) to show the presence of superstructure spots. The sublattice corresponds to an orthorhombic phase of $a = 5.5$, $b = 5.7$, $c = 14.9$ Å. In this case the modulation vector is $1/3\ b^*$ but it was not possible to determine the space group of the superstructure because of double diffraction problems. Diffraction patterns in the $(00\bar{1})^*$ and $(30\bar{1})^*$ planes of the $\beta$ phase (Figs. 3d and 3e) also show the presence of additional spots characterizing a superstructure. The substructure can be indexed with the orthorhombic lattice parameters $a = 5.5$, $b = 5.5$, and $c = 15.5$ Å. In this case, the modulation reoccurs along the $b^*$ axis with a vector $2/3\ b^*$. The diffraction pattern in the $(10\bar{1})^*$ plane of the $\gamma$ phase (Fig. 3f) clearly indicates the absence of modulation. The structure is indexed with parameters $a = 5.5$, $b = 5.5$, and $c = 15.5$ Å of a pseudotetragonal lattice.

The single crystal X-ray investigation of $\gamma$-$Bi_4V_2O_{10}$ has been briefly presented (5). The crystallographic parameters are summarized in Table 2, the atomic parameters are listed in Table 3, and the selected distances are shown in Table 4. The typical layered structure, containing $(Bi_2O_2)_{2n}$ layers alternating with $(VO_3)_{2n}$ ones, is schematically depicted in Fig. 4. This view is a particular case of the disorder affecting the $VO_5$ square pyramids in the $(VO_3)_{2n}$ layers. Indeed, vanadium and oxygen associated atoms are all distributed over two sites, giving several possibilities for $VO_5$ SP, above and below on either side of the mean basal plane, without a periodic order.

In this structure, the $(Bi_2O_2)_{2n}$ layers are well-defined with two independent bismuth atoms associated with four oxygen atoms, O1, O2, O3, O4, forming square planes. In particular, the Bi–O bonds are relatively similar: 2.25 to 2.43 Å (Table 4). Coordination is completed by other half-oxygen atoms corresponding to different O5, O6, O7 atoms (i.e., O51, O52, O61, O62, O71, O72 sites) (Fig. 5). The eleven atomic positions of near oxygen atoms around the Bi atoms (<3.2 Å) form a spheric envelope whose center coordinates are $x_1 = 0.27$, $y_1 = 0.77$, $z_1 = 0.13$ for $E1$ and $x_2 = 0.22$, $y_2 = 0.68$, $z_2 = 0.37$ for $E2$, i.e., at 0.80 Å and 0.85 Å of Bi1 and Bi2 atoms, respectively. $E1$ and $E2$ represent the center of the "spherical" influence zone of

**TABLE 2**
**Crystallographic Parameters of $\gamma Bi_4V_2O_{10}$**

| | |
|---|---|
| Crystal data | |
| Formula | $Bi_2VO_5$ |
| Crystal system | orthorhombic |
| Space group | $P2_1\ 2\ 2_1$ (No. 18) |
| $a$[Å] | 5.494(2) |
| $b$[Å] | 5.504(3) |
| $c$[Å] | 15.449(3) |
| $V$[Å]$^3$ | 467.1(3) |
| $Z$ | 4 |
| Molecular weight | 548.9 |
| $\rho$ calc [g/cm$^3$] | 7.81 |
| $\mu$[Mo$K\alpha$ cm$^{-1}$] | 742 |
| Morphology | platelet |
| Color | black |
| Dimension (mm) | 0.15 × 0.125 × 0.014 |
| Transmission factor range | 0.012–0.340 |
| Data collection | |
| Temperature [°C] | 20 |
| Wavelength [Mo$K\alpha$][Å] | 0.71069 |
| Monochromator | graphite |
| Scan mode | $\omega - 2\theta$ |
| Scan width [°] | 0.90 + 0.35 tan $\theta$ |
| Takeoff angle [°] | 3.5 |
| Max Bragg angle [°] | 35 |
| $T_{max.}$ [s] | 60 |
| Control reflections: | |
| Intensity (every 3600 s) | 0 2 6 / 0 0 12 / 1 1 9 |
| Orientation (every 150 refl.) | 1 1 5 / 2 2 6 |
| Structure refinement | |
| Reflections for cell refinement | 25 with $6° \le \theta \le 18°$ |
| Reflections collected | 1270 |
| Reflections unique measured | 583 |
| Reflections unique used | 583 |
| Parameters refined | 59 |
| Weighting | $w = 1$ |
| $R = \Sigma\|\|F_o\| - \|F_c\|\|/\Sigma\|F_o\|$ | 0.109 |
| $R_w = [\Sigma_w(\|F_o\| - \|F_c\|)^2/\Sigma wF_0^2]^{1/2}$ | 0.111 |

the lone pair of electrons associated with the bismuth cations in their valence state +III.

In contrast, vanadium atoms are less well-localized (Fig. 6). Statistically they are distributed over two sites V1 and V2 around 1/4, 1/4, 1/4. The crystallographic sites are separated by 0.6 Å and therefore are only 50% occupied. The oxygen atom environment also exhibits a disorder with half occupied sites O51, O52, O61, O62, O71, and O72. The resulting vanadium environment is built up by distorted square pyramids with apical corners either above or below the basal plane, V1 O71 $(O51)_2$ O61 O62 (Fig. 6a), toward trigonal bipyramid (TBP), V2 O72 $(O52)_2$ O62 O61 (Fig. 6b). These pyramid bases are linked and make up puckered layers with an angular distortion of 13° compared to the flat regular $(Bi_2O_2)_{2n}$ layers. The V1–O71 and V2–O72 distances indicate the presence of vanadyl groups. Despite such short V=O bonds, the parameter $c$ (15.449 Å) in the $\gamma$ $Bi_4V_2O_{10}$ phase is significantly larger than in the $Bi_4V_2O_{11}$ phase (15.254 Å). The atomic disorder in the $(VO_3)_{2n}$ layers, together with the influence of the lone pair of the bismuth atoms, increasing the stereochemical activity in accordance with the lower concentration of oxygen in the vanadium sheets, appears responsible for this effect. Moreover, if this disorder would increase with temperature, then the superstructure would not be observed in the $\gamma Bi_4V_2O_{10}$ phase.

### *$Bi_4V_{2y}O_{4y+6}$ or $(Bi_2O_2)_2V_{2y}O_{4y+2}$ ($1 < y \le 4$)*

The XPD spectra of the phases corresponding to $y = 2$, 3, 4 obtained are closely related (Fig. 7). They have been indexed on the basis of the $Bi_4V_2O_{10}$ ($y = 1$) orthorhombic cell (Fig. 7, Table 1). There is a smooth evolution of the cell parameters but parameters $a$ and $b$ tend to be become more equal, the orthorhombic structure becoming quasi-tetragonal as $y$ increases.

Since the phases $Bi_4V_{2y}O_{4y+6}$ when $y > 1$ decompose before melting, only powder samples were available (attempts to make definite single crystals for $y = 2$, 3, or 4 have failed). An analogy of the structures of $Bi_4V_{2y}O_{4y+6}$ with $y$ varying continuously from $y = 1$ to $y = 4$ can be made with the structural organization of the series $CaV_nO_{2n+1}$ (6) (Fig. 8). In these latter compounds, $(V_2O_5)_n$, $(V_3O_7)_n$, and $(V_4O_9)_n$ layers alternate with calcium layers. Based also on our knowledge of the structure of the $Bi_4V_2O_{10}$ phase (Fig. 4), it is reasonable to assume that the layered structure in the series $Bi_4V_{2y}O_{4y+6}$ would be built up by $(Bi_2O_2)_{2n}$ layers alternating with $(V_{2y}O_{4y+2})_n$ ones.

If the $(Bi_2O_2)_{2n}$ layers have the same organization and roughly the same parameters along the $a$ and $b$ directions, the $(V_{2y}O_{4y+2})_n$ layers undergo a drastic rearrangement due to: the evolution of stoichiometry, when $y$ increases from $y = 1$ to $y = 4$, accommodated by a continuous densification of the $(V_{2y}O_{4y+2})_n$ layer (increasingly $VO_5$ square pyramids share edges); and the topological distorsions introduced by the difference in size of the square base of the $VO_5$ and $BiO_4E$ square pyramids, i.e. ~ 7.9 and 8.5 Å$^2$, respectively.

In Fig. 9a, an idealized perspective view of the structure of such $(Bi_2O_2)_2V_{2y}O_{4y+2}$ compounds is given, with different $(V_{2y}O_{4y+2})_n$ layers, which are not compulsorily built up by the same arrangement of $VO_5$ square pyramids. The misfit between the pavement of the $VO_5$ and $BiO_4E$ square pyramids is clearly shown in the idealized projection onto the plane (001) of Fig. 9b. A tentative picture of what could happen if the $(V_{2y}O_{4y+2})_n$ layers adapt to the space between the bismuth layers is illustrated in Fig. 9c, some puckerings of this layer being equally likely to occur. We suggest that the $(V_{2y}O_{4y+2})_n$ layer can be twisted in order to match the planar space between $(Bi_2O_2)_{2n}$ layers. For a

**TABLE 3**
**Atomic Parameters of $\gamma Bi_4V_2O_{10}$**

| Atom | $x$ | $y$ | $z$ | $\tau$ | $B^*_{eq.}$ *or* $B_{iso}$ (Å$^2$) |
|---|---|---|---|---|---|
| Bi1 | 0.248(2) | 0.749(1) | 0.0827(4) | 1 | 2.2(2)* |
| Bi2 | 0.239(1) | 0.7408(8) | 0.4193(3) | 1 | 1.0(1)* |
| V1 | 0.228(4) | 0.198(3) | 0.249(3) | 0.5 | 0.4(2) |
| V2 | 0.313(5) | 0.267(8) | 0.259(2) | 0.5 | 0.5(3) |
| O1 | 0 | −0.02(2) | 1/2 | 1 | 2.(1) |
| O2 | 1/2 | 0.02(2) | 1/2 | 1 | 2.(1) |
| O3 | 0 | 0.49(2) | 1/2 | 1 | 2.(1) |
| O4 | 1/2 | 0.52(1) | 1/2 | 1 | 1.(1) |
| O51 | 0.05(2) | −0.10(2) | 0.26(1) | 0.5 | 2.(1) |
| O52 | 0.05(2) | 0.00(2) | 0.30(1) | 0.5 | 3.(2) |
| O61 | 0.10(1) | 0.55(1) | 0.234(6) | 0.5 | 1.(1) |
| O62 | 0.01(1) | 0.50(2) | 0.278(5) | 0.5 | 1.(1) |
| O71 | 0.26(2) | 0.29(1) | 0.344(5) | 0.5 | 0.8(8) |
| O72 | 0.21(1) | 0.14(1) | 0.175(5) | 0.5 | 0.7(9) |

| Atom | $U11$ | $U22$ | $U33$ | $U12$ | $U13$ | $U23$ |
|---|---|---|---|---|---|---|
| Bi1 | 0.032(3) | 0.030(3) | 0.023(3) | 0.004(7) | −0.004(2) | −0.007(4) |
| Bi2 | 0.014(2) | 0.011(1) | 0.011(2) | −0.004(3) | 0.002(1) | 0.002(2) |

$B_{eq.} = 8\pi^2/3$ trace $U$

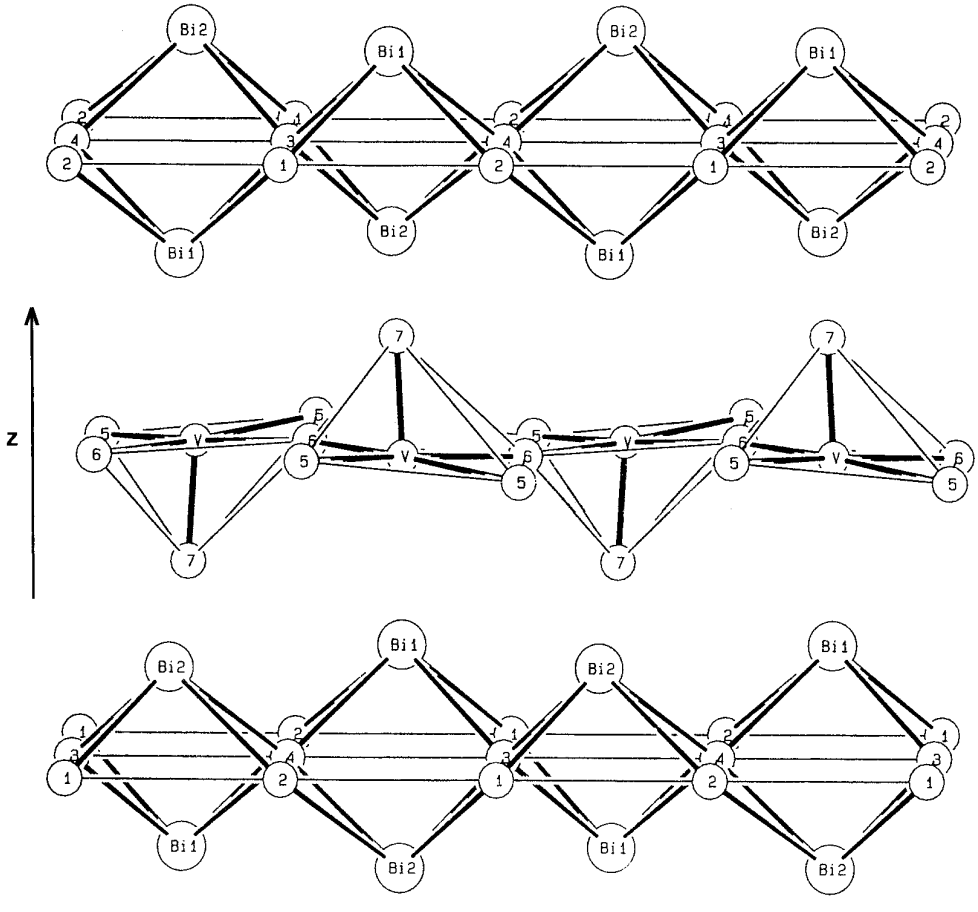


**FIG. 4.** Crystal structure of $\gamma Bi_4V_2O_{10}$: sequence of $(Bi_2O_2)_n$ and $(VO_3)_n$ layers.

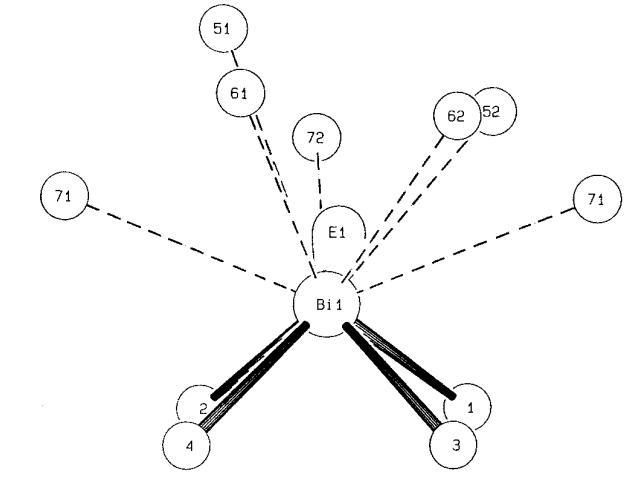


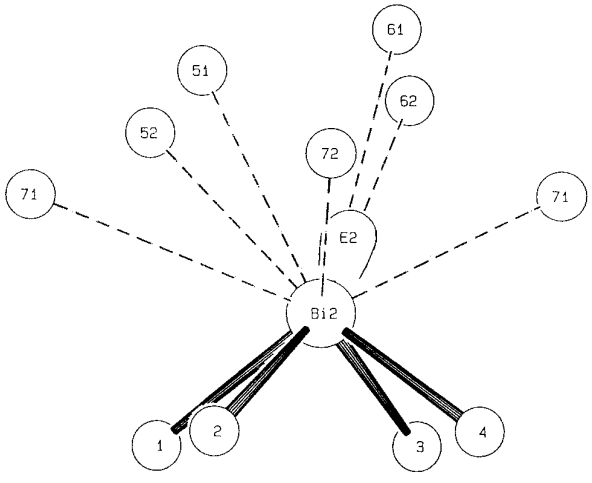


FIG. 5. Crystal structure of $\gamma Bi_4V_2O_{10}$: environment of the Bi atoms.

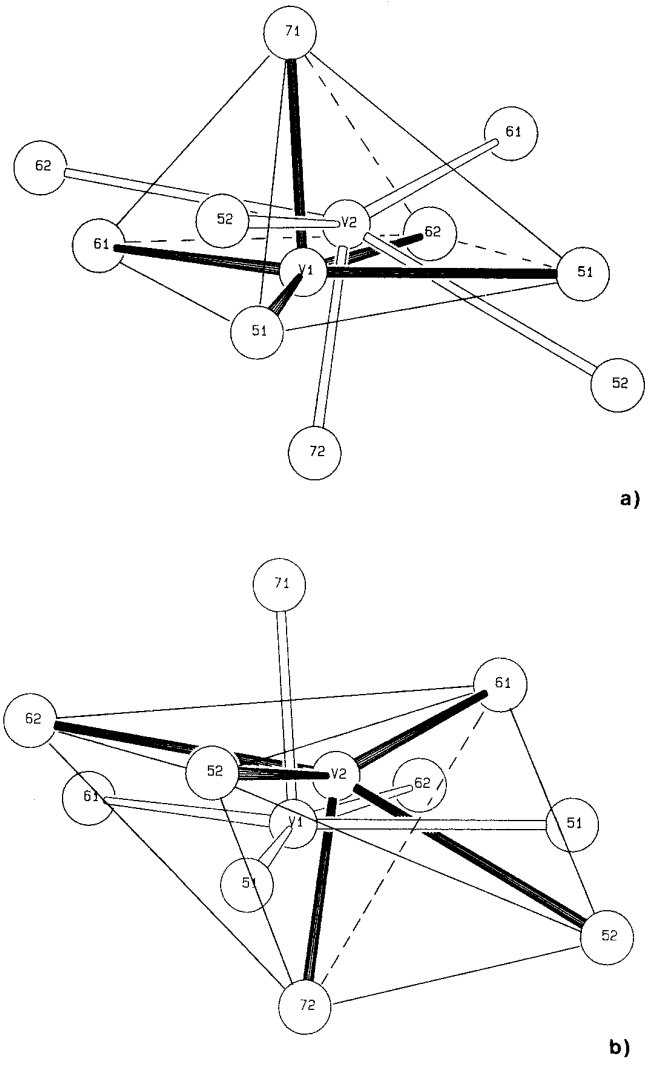


FIG. 6. Crystal structure of $\gamma Bi_4V_2O_{10}$: two types of environment of the V atoms, (a) square pyramid and (b) trigonal bipyramid.

**TABLE 4**
**Selected Interatomic and Intersites(*) Distances (Å) in $\gamma Bi_4V_2O_{10}$**

| | | | |
|---|---|---|---|
| Bi1–O1 | 2.41(5) | Bi2–O1 | 2.24(5) |
| O2 | 2.28(4) | O2 | 2.43(5) |
| O3 | 2.30(4) | O3 | 2.27(4) |
| O4 | 2.39(5) | O4 | 2.25(4) |
| O72 | 2.58(6) | O52 | 2.52(6) |
| O61 | 2.70(6) | O51 | 2.76(7) |
| O52 | 2.79(7) | O71 | 2.76(6) |
| O71 | 2.91(6) | O62 | 2.84(7) |
| V1–O51 | 1.86(8) | V2–O52 | 2.16(10) |
| O51 | 1.91(9) | O52 | 2.19(8) |
| O61 | 2.09(7) | O61 | 1.87(8) |
| O62 | 2.31(7) | O62 | 2.09(8) |
| O71 | 1.56(7) | O72 | 1.59(7) |
| *V1 ⋯ V2 | 0.63(3) | *O51 ⋯ O52 | 0.8(2) |
| | | *O61 ⋯ O62 | 0.9(1) |

sake of clarity the $(V_{2y}O_{4y+2})_n$ layer is represented in Fig. 9c with only $VO_5$ SP sharing corners, but of course it can be more dense with increasing $y$ values.

### *Phase Relationships in the $Bi_2O_3$–$V_2O_m$ ($m = 3, 4, 5$) Systems*

In order to arrive at a consistent interpretation of the study of the $VO_2$-rich side of the $Bi_2O_3$–$V_2O_4$ system, it is necessary to compare the results with those recorded in the $Bi_2O_3$–$V_2O_3$ and $Bi_2O_3$–$V_2O_3$ systems.

In the $Bi_2O_3$–$V_2O_5$ system, numerous investigations have been reported, in particular $BiVO_4$ (13) with scheelite structure and $Bi_4V_2O_{11}$ (5) (14–16) with an Aurivillius structure type. The vanadium V cations exhibit two coordination polyhedra, tetrahedral and octahedral, respectively.

To our knowledge, in the $Bi_2O_3$–$V_2O_3$ system there is no literature data. Studies of the $V_2O_3$-rich side of the $(1-y)Bi_2O_3 + yV_2O_3$ system show that an oxido-reduction process takes place. The mixture of the three phases "$Bi_4V_2O_9$", $Bi_{1.66}V_8O_{16}$, and Bi° has been produced. The comparison of "$Bi_4V_2O_9$" and $Bi_4V_2O_{10}$ reveals significantly similar unit cell parameters. The partial oxidation of $V^{III}$ to $V^{IV}$ appears as a very likely explanation in this case. Otherwise, the preparation of $Bi_{1.66}V_8O_{16}$ as a single phase strongly depends on the proportion of starting oxides. A tetragonal phase, mixture of $V^{III}$ and $V^{IV}$, according to the formula $1.66Bi_2O_3 + 5V_2O_3 + 6VO_2 \rightarrow 2Bi_{1.66}V_8O_{16}$ has been obtained. Unit cell parameters $a = 9.935(2)$, $c = 2.915(2)$ Å and the hollandite structure type are in agreement with the results of Abraham and Mentre (12). Finally, a phase containing only $Bi^{III}$ and $V^{III}$ does not seem to exist.

Thus, there are many differences between the $Bi_2O_3$–$V_2O_3$, $Bi_2O_3$–$V_2O_4$, and $Bi_2O_3$–$V_2O_5$ systems. These result from the ability of vanadium atoms to exhibit several oxidation states, $V^{III}$, $V^{IV}$, $V^{V}$, associated with the great flexibility in the coordination polyhedra in the case of two last cations.

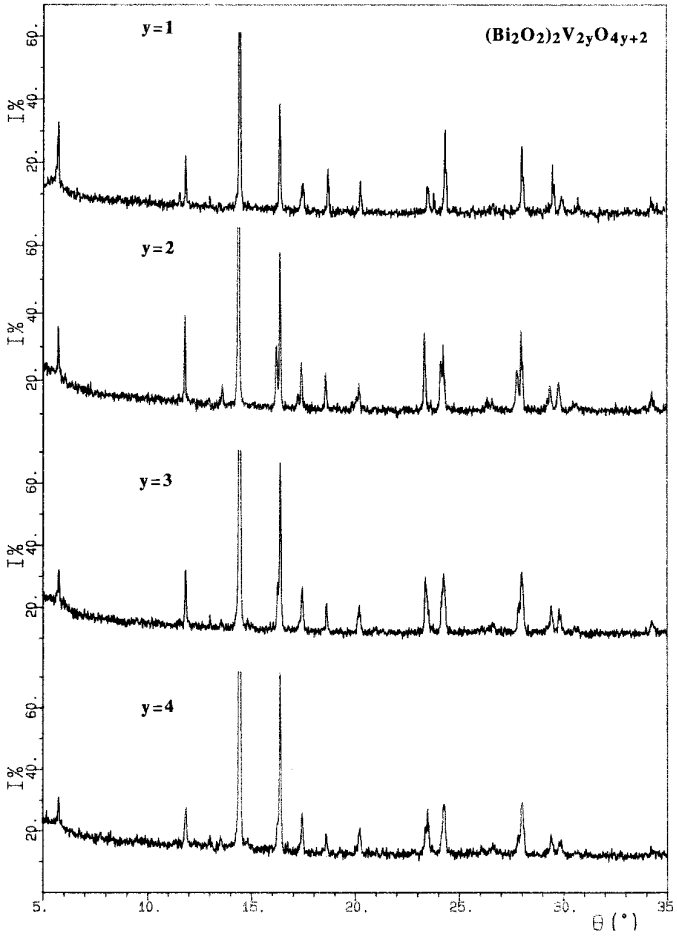


**FIG. 7.** X-ray powder diffraction patterns of $(Bi_2O_2)_2V_{2y}O_{4y+2}$ ($y$ = 1, phase at 890°C and $y$ = 2, 3, 4, phases at 650°C).

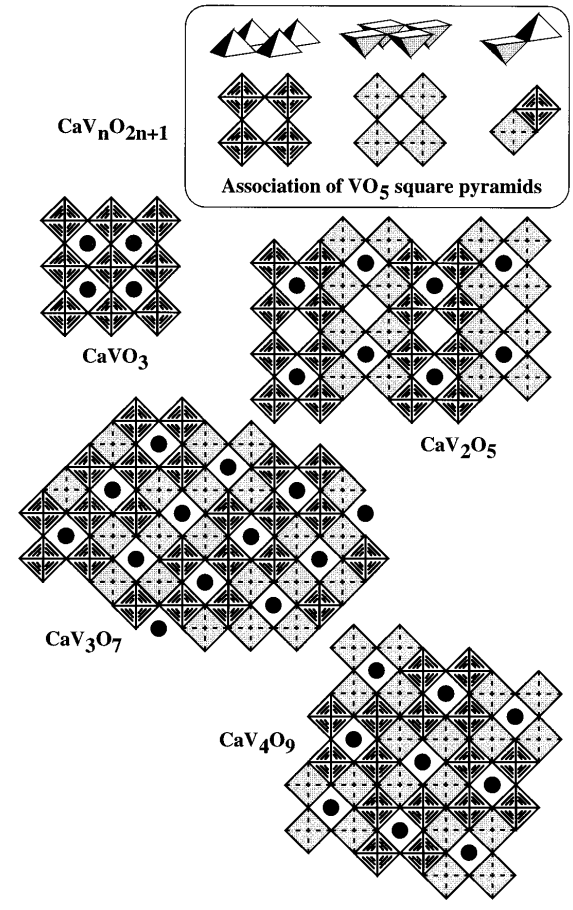


**FIG. 8.** Representation of the structures of the $Ca_nV_nO_{2n+1}$ series.

## CONCLUSION

The $Bi_4V_{2y}O_{4y+6}$ phases with $1 \leq y \leq 4$ are an example of the remarkable potential of the vanadate IV layers to adopt (via distortions of the fivefold oxygen square pyramids surrounding the vanadium atoms, condensation, rotations, and puckering) the periodicity imposed by $(Bi_2O_2)_{2n}$ layers. Again, as in $Bi_4V_2O_{11}$, these results confirm that the disorder occurs in the vanadium–oxygen layer and more precisely affects the oxygen atoms in the basal plane and not just at the level of the apical positions of the pyramids. This phenomenon strongly supports the diffusion of oxygen atoms in this plane as shown by Pernot (16), this diffusion being responsible for the ionic conductivity in the $Bi_4V_2O_{11}$ phase and also in the $Bi_4V_2O_{11-x}$ series.

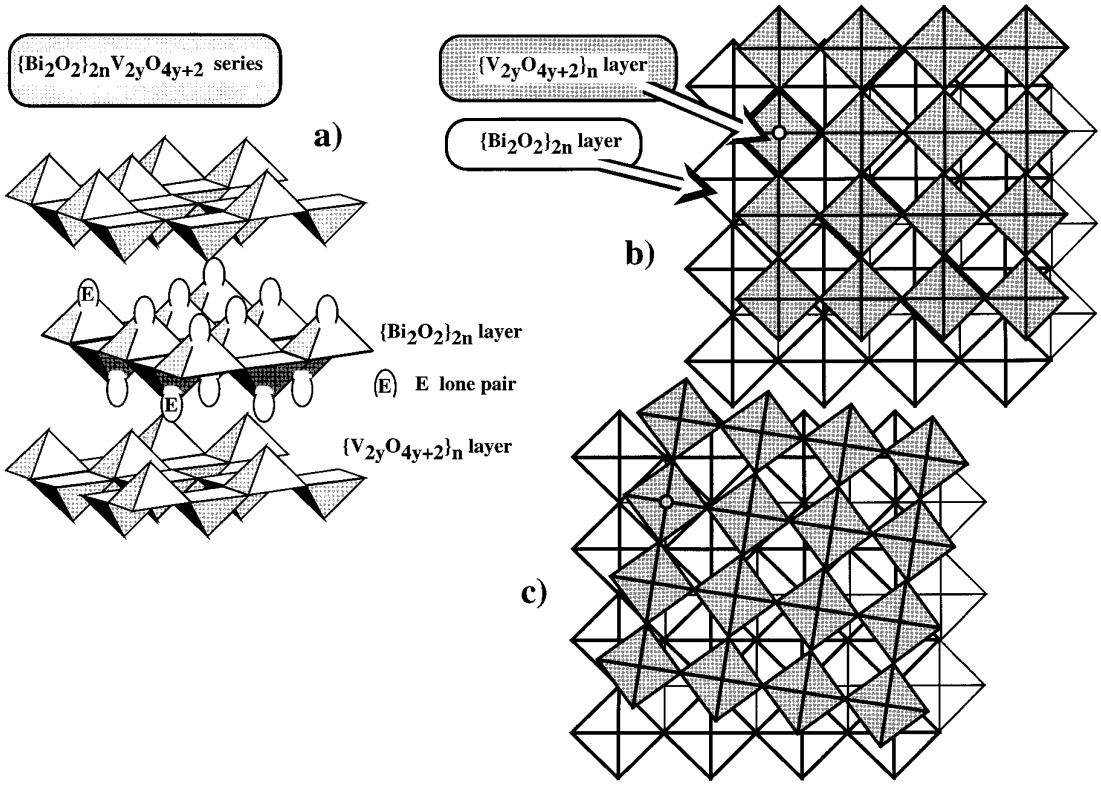


**FIG. 9.** Idealized representation in the $(Bi_2O_2)_2V_{2y}O_{4y+2}$ series: (a) $(Bi_2O_2)_{2n}V_{2y}O_{4y+2}$ multilayer phases built up by an intergrowth of $(Bi_2O_2)_{2n}$ and $(V_{2y}O_{4y+2})_n$ layers; (b) misfit between the pavements of the bases of the $VO_5$ square pyramids and $BiO_4E$; (c) possible adjustment of the $(V_{2y}O_{4y+2})_n$ layer to fit with the larger pavement of the $(Bi_2O_2)_{2n}$ layer.

## REFERENCES


1. J. Galy, G. Meunier, S. Andersson, and A. Åstrom, *J. Solid State Chem.* **13,** 142 (1975).
2. J. Galy and R. Enjalbert, *J. Solid State Chem.* **44,** 1 (1982).
3. B. Frit, G. Roult, and J. Galy, *J. Solid State Chem.* **48,** 246 (1983).
4. J. Galy, *J. Solid State Chem.* **100,** 229 (1992).
5. J. Galy, R. Enjalbert, P. Millan, and A. Castro, *C.R. Acad. Sci. Paris II* **317,** 43 (1993).
6. J. C. Bouloux and J. Galy, *J. Solid State Chem.* **16,** 385 (1976).
7. J. C. Bouloux and J. Galy, *Acta Crystallogr. Sect. B* **29,** 1335 (1973).
8. J. C. Bouloux and J. Galy, *Acta Crystallogr. Sect. B* **29,** 269 (1973).
9. G. Liu and J. E. Greedan, *J. Solid State Chem.* **115,** 174 (1995).
10. A. Ramanan, J. Gopalakrishnan, and C. N. R. Rao, *J. Solid State Chem.* **60,** 376 (1985).
11. K. B. R. Varma, G. N. Subbanna, T. N. Guru Row, and C. N. R. Rao, *J. Mater. Res.* **5,** 2718 (1990).
12. F. Abraham and O. Mentre, *J. Solid State Chem.* **109,** 127 (1994).
13. A. W. Sleight, H. Y. Chen, A. Ferretti, and D. E. Cox, *Mater. Res. Bull.* **14,** 1571 (1979).
14. F. Abraham, M. F. Debreuille-Gresse, G. Mairesse, and G. Nowogrocki, *Solid State Ionics* **28,** 529 (1988).
15. O. Joubert, A. Jouanneaux, and M. Ganne, *J. Mater. Res.* **2,** 175 (1994).
16. E. Pernot, Thesis of University Grenoble, 1994.